

## Swift Observations of GRB 100424A

*E. A. Hoversten (PSU), P. A. Curran (MSSL-UCL), M. C. Stroh (PSU), D. Grupe(PSU), H. A. Krimm (GSFC/USRA), S. D. Barthelmy (GSFC), D. N. Burrows (PSU), P. W. A. Roming (PSU), & N. Gehrels (GSFC) for the Swift Team*

### 1 Introduction

At 16:32:42 UT on 24 April 2010 BAT triggered on and located GRB 100424A (Hoversten, *et al.*, *GCN Circ.* 10667, Trigger #420367). Swift slewed to this burst immediately. XRT began follow up observations at  $T + 126$  s, and UVOT observations began at  $T + 128$  s. Our best position is the UVOT-enhanced XRT position at  $RA(J2000) = 209.44775$  deg (13h57m47.46s),  $Dec(J2000) = +1.53897$  deg (+01d32'20.3'') with an uncertainty of 1.7 arcsec (radius, 90% confidence). The afterglow was not detected by UVOT.

Ground-based observations of GRB 100424A were reported by numerous observatories. Gemini/NIRI detected the afterglow in the  $J$  and  $K$  bands at  $T + 14$  hrs (Cenko, *et al.*, *GCN Circ.* 10682) and confirmed that it was fading at  $T + 17$  hrs (Cenko, *et al.*, *GCN Circ.* 10690). The spectral shape indicated that the red colors were due to large reddening rather than a large redshift. The CrAO observatory report the detection of a source in the  $R$  band 2.8'' from the XRT position, but do not see a source at the Gemini position (Rumyantsev, *et al.*, *GCN Circ.* 10693). Optical non detections were reported by NOT (Malesani, *et al.*, *GCN Circ.* 10671), WHT (Levan, *et al.*, *GCN Circ.* 10672), PAIRITEL (Morgan, *et al.*, *GCN Circ.* 10675), GROND (Olivares, *et al.*, *GCN Circ.* 10676), Lulin (Huang, *et al.*, *GCN Circ.* 10677), MITSuME (Kuroda, *et al.*, *GCN Circ.* 10679), D50 (Strobl, *et al.*, *GCN Circ.* 10681), and Liverpool Telescope (Cano, *et al.*, *GCN Circ.* 10687). The afterglow was not detected at 8.46 GHz (Frail & Chandra, *GCN Circ.* 10701).

### 2 BAT Observation and Analysis

Using the data set from  $T - 60$  to  $T + 243$  s further analysis of GRB 100424A (trigger #420367) was performed by the Swift team (Krimm, *et al.*, *GCN Circ.* 10667). The BAT ground-calculated position is  $RA(J2000) = 209.453$  deg (13h57m48.6s),  $Dec(J2000) = +1.512$  deg (+01d30'44.2'') with an uncertainty of 1.5 arcmin, (radius, sys+stat, 90% containment). The partial coding was 88%.

The mask-weighted light curve shows a single broad peak from about  $T + 20$  to  $T + 150$  s.  $T_{90}$  (15 – 350keV) is  $104 \pm 15$  s (estimated error including systematics).

The time-averaged spectrum from  $T + 22.3$  to  $T + 148.5$ s is best fit by a simple power-law model. The power law index of the time-averaged spectrum is  $1.83 \pm 0.13$ . The fluence in the 15-150 keV band is  $1.5 \pm 0.1 \times 10^{-6}$  erg  $cm^{-2}$ . The 1-second peak photon flux measured from  $T + 58.28$  s in the 15-150 keV band is  $0.4 \pm 0.1$  photon  $cm^{-2} s^{-1}$ . All the quoted errors are at the 90% confidence level.

The BAT light curve is shown in Figure 1.

### 3 XRT Observations and Analysis

The UVOT-enhanced XRT position of GRB 100424A is  $RA(J2000) = 209.44775$  deg (13h57m47.46s),  $Dec(J2000) = +1.53897$  deg (+01d32'20.3'') with an uncertainty of 1.7 arcsec (radius, 90% confidence, Evans, *et al.*, *GCN Circ.* 10669). This position is within 1.5 arcsec of the near infrared position reported by Cenko, *et al.*, *GCN Circ.* 10682.

XRT observations began 126 seconds after the BAT trigger. Analysis of 641 s of XRT data from 126

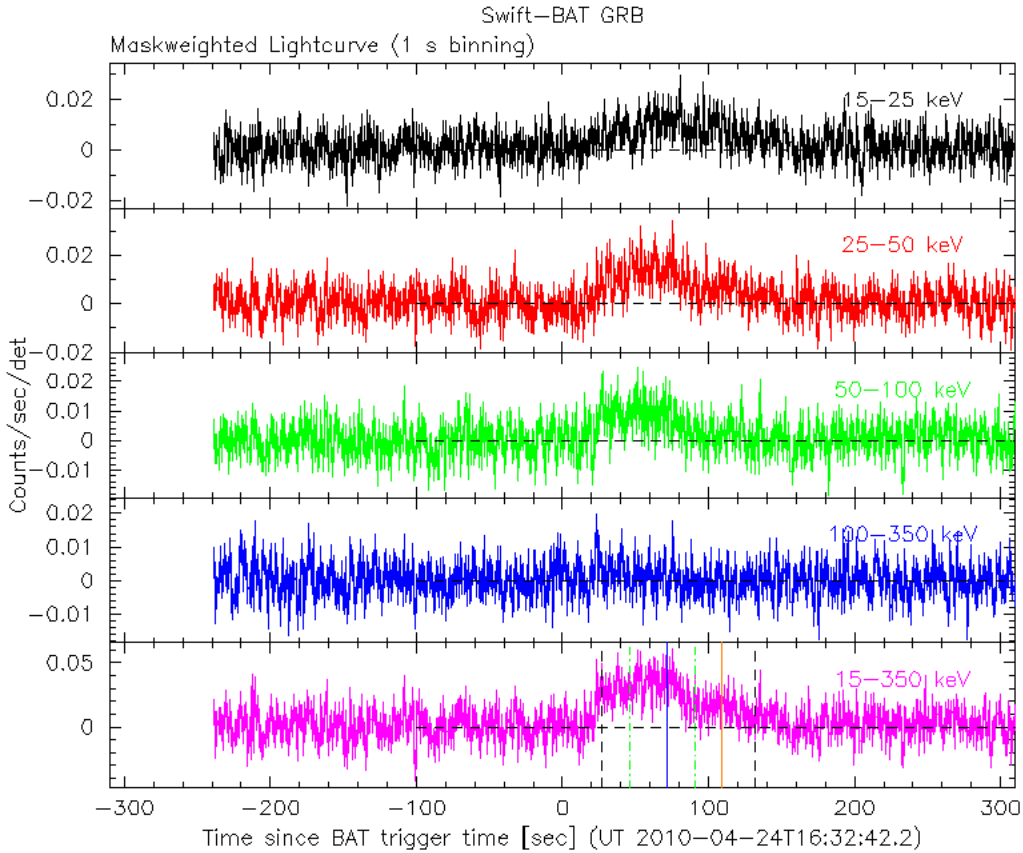


Figure 1: BAT Light curve. The mask-weighted light curve over all energy bands. The units are counts/s/illuminated-detector (note illum-det =  $0.16 \text{ cm}^2$ ) and  $T_0$  is 16:32:42.2 UT.

to 769 s after the BAT trigger was performed (Stroh, *et al.*, *GCN Circ.* 10674). The data comprise of 509 s in Windowed Timing (WT) mode with the remainder in Photon Counting (PC) mode. The light curve can be modeled with a series of power-law decays. The initial decay index is  $\alpha = 0.63 \pm 0.14$ . At  $T + 288 \text{ s}$  the decay steepens to  $\alpha = 1.41^{+0.27}_{-0.19}$  before breaking again at  $T + 526 \text{ s}$  to a final decay with index  $\alpha = 2.8^{+0.9}_{-0.6}$ .

A spectrum formed from the WT mode data can be fitted with an absorbed power-law with a photon spectral index of  $1.26 \pm 0.06$ . The best-fitting absorption column is  $1.62^{+0.22}_{-0.21} \times 10^{21} \text{ cm}^{-2}$ , in excess of the Galactic value of  $2.3 \times 10^{20} \text{ cm}^{-2}$  (Kalberla *et al.* 2005). The counts to observed (unabsorbed) 0.3-10 keV flux conversion factor deduced from this spectrum is  $5.8 \times 10^{-11}$  ( $6.5 \times 10^{-11}$ )  $\text{erg cm}^{-2} \text{ count}^{-1}$ .

The XRT light curve is shown in Figure 2.

## 4 UVOT Observation and Analysis

The Swift/UVOT began settled observations of the field of GRB 100424A 128 s after the BAT trigger (Curran & Hoversten, *GCN Circ.* 10688). No optical afterglow consistent with the UVOT-enhanced XRT position or at the position of the NIR counterpart (Cenko, *et al.*, *GCN Circ.* 10682) is detected in the UVOT exposures. Upper limits are summarized in Table 1. The magnitudes reported in the table are on the UVOT Photometric System (Poole *et al.*, 2008, *MNRAS* 383,627). They are

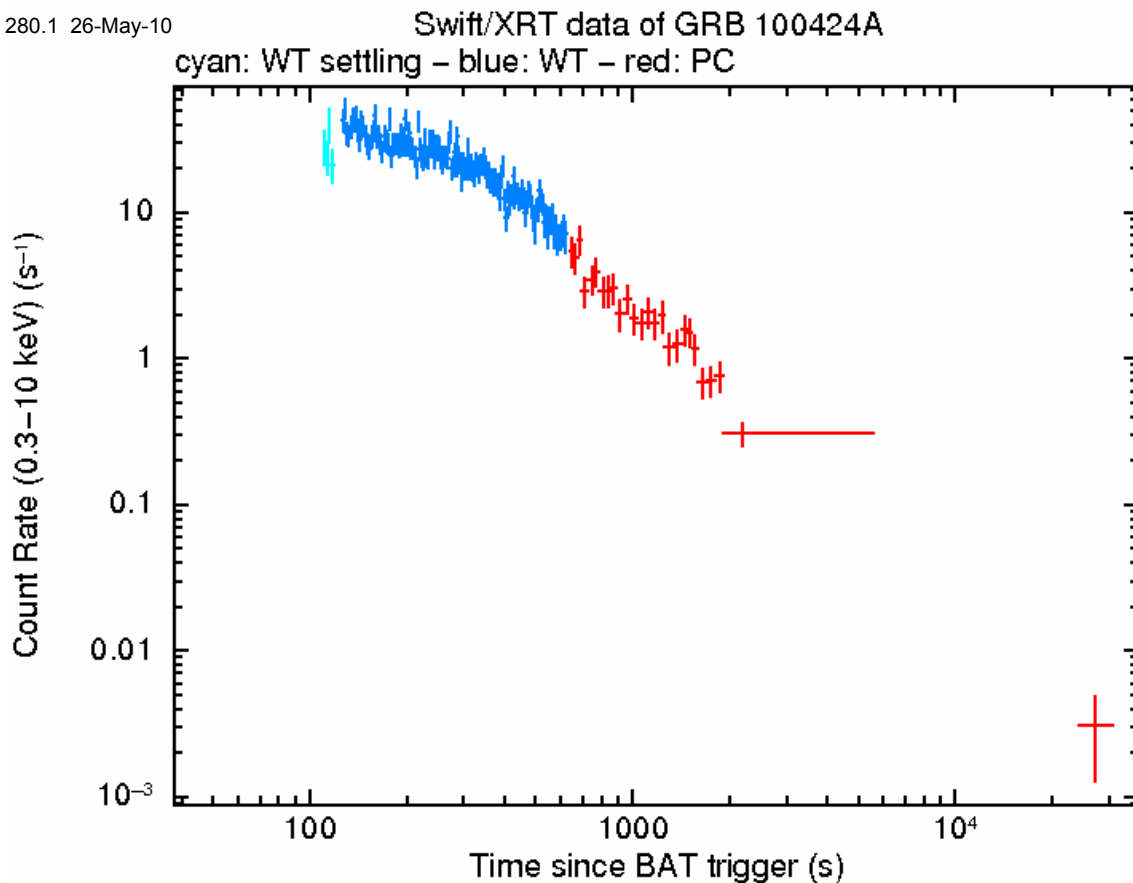


Figure 2: XRT Light curve. Flux in the 0.3-10 keV band: settling exposure (cyan), Window Timing Mode (blue), and Photon Counting mode (red). The approximate conversion is  $1 \text{ count s}^{-1} \simeq 5.8 \times 10^{-11} \text{ ergs cm}^{-2} \text{ s}^{-1}$ .

not corrected for Galactic extinction which is  $E(B - V) = 0.08$  along the line of sight to the burst (Schlegel, Finkbeiner, & Davis, 1998).

## References

- [1] Cano, Z., et al. 2010, *GCN Circ.* 10687
- [2] Cenko, S. B., et al. 2010, *GCN Circ.* 10682
- [3] Cenko, S. B., et al. 2010, *GCN Circ.* 10690
- [4] Curran, P. A. & Hoversten, E. A. 2010, *GCN Circ.* 10688
- [5] Evans, P. A., et al. 2010, *GCN Circ.* 10669
- [6] Frail, D. A. & Chandra, P. 2010, *GCN Circ.* 10701
- [7] Hoversten, E. A., et al. 2010, *GCN Circ.* 10667
- [8] Huang, K. Y., et al. 2010, *GCN Circ.* 10677
- [9] Kalberla, P. M. W., et al. 2005, *A. & A.*, 440, 775
- [10] Krimm, H. A., et al. 2010, *GCN Circ.* 10670

- [11] Kuroda, D., et al. 2010, *GCN Circ.* 10679
- [12] Levan, A. J., et al. 2010, *GCN Circ.* 10672
- [13] Malesani, D., et al. 2010, *GCN Circ.* 10671
- [14] Morgan, A. N. & Bloom, S. J. 2010, *GCN Circ.* 10675
- [15] Olivares, F., et al. 2010, *GCN Circ.* 10676
- [16] Poole, T. S., et al. 2008, *MNRAS*, 383, 627
- [17] Rumyantsev, V., et al. 2010, *GCN Circ.* 10693
- [18] Schlegel, D. J., Finkbeiner, D., & Davis, M. 1998, *ApJ.*, 500, 525
- [19] Strobl, J., et al. 2010, *GCN Circ.* 10681
- [20] Stroh, M. C., et al. 2010, *GCN Circ.* 10674

Filter	Start	Stop	Exposure	Magnitude
white	128	278	147	> 20.8 (FC)
<i>u</i>	288	537	246	> 20.0 (FC)
white	128	2046	444	> 21.2
<i>v</i>	618	1930	156	> 19.2
<i>b</i>	543	2028	156	> 20.1
<i>u</i>	288	2003	382	> 20.1
uvw1	668	1979	156	> 19.7
uvm2	642	1955	97	> 19.1
uvw2	594	5584	193	> 20.0

Table 1: UVOT observations